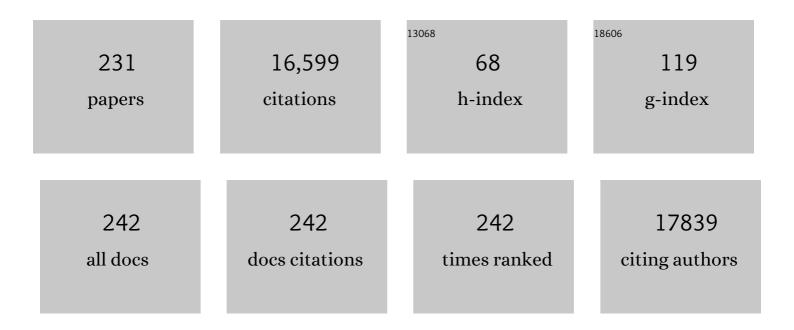
List of Publications by Year in descending order

Source: https://exaly.com/author-pdf/4405772/publications.pdf Version: 2024-02-01



#	Article	IF	CITATIONS
1	Shape-Controlled Synthesis of Pd Nanocrystals and Their Catalytic Applications. Accounts of Chemical Research, 2013, 46, 1783-1794.	7.6	568
2	Low Temperature Synthesis of Flowerlike ZnO Nanostructures by Cetyltrimethylammonium Bromide-Assisted Hydrothermal Process. Journal of Physical Chemistry B, 2004, 108, 3955-3958.	1.2	484
3	Enhancing the catalytic and electrocatalytic properties of Pt-based catalysts by forming bimetallic nanocrystals with Pd. Chemical Society Reviews, 2012, 41, 8035.	18.7	481
4	Synthesis of Pd nanocrystals enclosed by {100} facets and with sizes <10 nm for application in CO oxidation. Nano Research, 2011, 4, 83-91.	5.8	436
5	Platinum Concave Nanocubes with Highâ€Index Facets and Their Enhanced Activity for Oxygen Reduction Reaction. Angewandte Chemie - International Edition, 2011, 50, 2773-2777.	7.2	414
6	Nobleâ€Metal Nanocrystals with Concave Surfaces: Synthesis and Applications. Angewandte Chemie - International Edition, 2012, 51, 7656-7673.	7.2	411
7	Shapeâ€Controlled Synthesis of Copper Nanocrystals in an Aqueous Solution with Glucose as a Reducing Agent and Hexadecylamine as a Capping Agent. Angewandte Chemie - International Edition, 2011, 50, 10560-10564.	7.2	410
8	Synthesis of Pdâ^'Pt Bimetallic Nanocrystals with a Concave Structure through a Bromide-Induced Galvanic Replacement Reaction. Journal of the American Chemical Society, 2011, 133, 6078-6089.	6.6	405
9	Palladium Concave Nanocubes with Highâ€Index Facets and Their Enhanced Catalytic Properties. Angewandte Chemie - International Edition, 2011, 50, 7850-7854.	7.2	379
10	Intermetallic Nanocrystals: Syntheses and Catalytic Applications. Advanced Materials, 2017, 29, 1605997.	11.1	375
11	Palladium nanocrystals enclosed by {100} and {111} facets in controlled proportions and their catalytic activities for formic acid oxidation. Energy and Environmental Science, 2012, 5, 6352-6357.	15.6	358
12	Controllable Growth of ZnO Microcrystals by a Capping-Molecule-Assisted Hydrothermal Process. Crystal Growth and Design, 2005, 5, 547-550.	1.4	320
13	Synthesis of flower-like ZnO nanostructures by an organic-free hydrothermal process. Nanotechnology, 2004, 15, 622-626.	1.3	290
14	Facile Synthesis of Pd–Pt Alloy Nanocages and Their Enhanced Performance for Preferential Oxidation of CO in Excess Hydrogen. ACS Nano, 2011, 5, 8212-8222.	7.3	236
15	Large-Scale Synthesis of SnO2 Nanotube Arrays as High-Performance Anode Materials of Li-Ion Batteries. Journal of Physical Chemistry C, 2011, 115, 11302-11305.	1.5	231
16	Controlling the Nucleation and Growth of Silver on Palladium Nanocubes by Manipulating the Reaction Kinetics. Angewandte Chemie - International Edition, 2012, 51, 2354-2358.	7.2	209
17	A simple hydrothermal route for synthesizing SnO2quantum dots. Nanotechnology, 2006, 17, 2386-2389.	1.3	202
18	Epitaxial Growth of Twinned Au–Pt Core–Shell Star-Shaped Decahedra as Highly Durable Electrocatalysts. Nano Letters, 2015, 15, 7808-7815.	4.5	195

#	Article	IF	CITATIONS
19	Controlling the Morphology of Rhodium Nanocrystals by Manipulating the Growth Kinetics with a Syringe Pump. Nano Letters, 2011, 11, 898-903.	4.5	190
20	Three-dimensional Dendritic Pt Nanostructures: Sonoelectrochemical Synthesis and Electrochemical Applications. Journal of Physical Chemistry C, 2008, 112, 16385-16392.	1.5	180
21	Porous ZnCo ₂ O ₄ Nanowires Synthesis via Sacrificial Templates: High-Performance Anode Materials of Li-Ion Batteries. Inorganic Chemistry, 2011, 50, 3320-3324.	1.9	178
22	Multiwalled Carbon Nanotubes Anchored with SnS ₂ Nanosheets as High-Performance Anode Materials of Lithium-Ion Batteries. ACS Applied Materials & Interfaces, 2011, 3, 4067-4074.	4.0	159
23	A selective NH3 gas sensor based on Fe2O3–ZnO nanocomposites at room temperature. Sensors and Actuators B: Chemical, 2006, 114, 910-915.	4.0	155
24	Kinetically controlled synthesis of Pt–Cu alloy concave nanocubes with high-index facets for methanol electro-oxidation. Chemical Communications, 2014, 50, 560-562.	2.2	140
25	CNTs@SnO ₂ @C Coaxial Nanocables with Highly Reversible Lithium Storage. Journal of Physical Chemistry C, 2010, 114, 22535-22538.	1.5	139
26	Copper Can Still Be Epitaxially Deposited on Palladium Nanocrystals To Generate Core–Shell Nanocubes Despite Their Large Lattice Mismatch. ACS Nano, 2012, 6, 2566-2573.	7.3	139
27	Controllable growth of ZnO nanostructures by citric acid assisted hydrothermal process. Materials Letters, 2005, 59, 1696-1700.	1.3	138
28	Ligand-free Self-Assembly of Ceria Nanocrystals into Nanorods by Oriented Attachment at Low Temperature. Journal of Physical Chemistry C, 2007, 111, 12677-12680.	1.5	137
29	<i>In Situ</i> Synthesis of Multilayer Carbon Matrix Decorated with Copper Particles: Enhancing the Performance of Si as Anode for Li-Ion Batteries. ACS Nano, 2019, 13, 3054-3062.	7.3	135
30	Carbon-coated SnO ₂ nanotubes: template-engaged synthesis and their application in lithium-ion batteries. Nanoscale, 2011, 3, 746-750.	2.8	131
31	CuO nanodendrites synthesized by a novel hydrothermal route. Nanotechnology, 2004, 15, 1428-1432.	1.3	122
32	In situ Study of Oxidative Etching of Palladium Nanocrystals by Liquid Cell Electron Microscopy. Nano Letters, 2014, 14, 3761-3765.	4.5	120
33	Nanocrystals Composed of Alternating Shells of Pd and Pt Can Be Obtained by Sequentially Adding Different Precursors. Journal of the American Chemical Society, 2011, 133, 10422-10425.	6.6	115
34	Coupling PtNi Ultrathin Nanowires with MXenes for Boosting Electrocatalytic Hydrogen Evolution in Both Acidic and Alkaline Solutions. Small, 2019, 15, e1805474.	5.2	113
35	Arrays of ZnO nanowires fabricated by a simple chemical solution route. Nanotechnology, 2003, 14, 423-426.	1.3	111
36	Highly loaded CoO/graphene nanocomposites as lithium-ion anodes with superior reversible capacity. Journal of Materials Chemistry A, 2013, 1, 2337.	5.2	111

#	Article	IF	CITATIONS
37	Aqueous Solution Synthesis of Pt–M (M = Fe, Co, Ni) Bimetallic Nanoparticles and Their Catalysis for the Hydrolytic Dehydrogenation of Ammonia Borane. ACS Applied Materials & Interfaces, 2014, 6, 12429-12435.	4.0	110
38	From cobalt nitrate carbonate hydroxide hydrate nanowires to porous Co ₃ O ₄ nanorods for high performance lithium-ion battery electrodes. Nanotechnology, 2008, 19, 035711.	1.3	105
39	Selective Synthesis of Fe2O3 and Fe3O4 Nanowires Via a Single Precursor: A General Method for Metal Oxide Nanowires. Nanoscale Research Letters, 2010, 5, 1295-1300.	3.1	105
40	Hydrothermal Synthesis of Zn2SnO4 Nanorods in the Diameter Regime of Sub-5 nm and Their Properties. Journal of Physical Chemistry B, 2006, 110, 7631-7634.	1.2	104
41	Self-Templating Synthesis of SnO ₂ –Carbon Hybrid Hollow Spheres for Superior Reversible Lithium Ion Storage. ACS Applied Materials & Interfaces, 2011, 3, 1946-1952.	4.0	104
42	Tuning Surface Structure and Strain in Pd–Pt Core–Shell Nanocrystals for Enhanced Electrocatalytic Oxygen Reduction. Small, 2017, 13, 1603423.	5.2	104
43	Gas sensing behavior of polyvinylpyrrolidone-modified ZnO nanoparticles for trimethylamine. Sensors and Actuators B: Chemical, 2006, 113, 324-328.	4.0	103
44	Epitaxial Growth of Multimetallic Pd@PtM (M = Ni, Rh, Ru) Core–Shell Nanoplates Realized by in Situ-Produced CO from Interfacial Catalytic Reactions. Nano Letters, 2016, 16, 7999-8004.	4.5	103
45	Single crystalline CdS nanorods fabricated by a novel hydrothermal method. Chemical Physics Letters, 2003, 377, 654-657.	1.2	102
46	Carbon Nanocapsules as Nanoreactors for Controllable Synthesis of Encapsulated Iron and Iron Oxides: Magnetic Properties and Reversible Lithium Storage. Journal of Physical Chemistry C, 2011, 115, 3612-3620.	1.5	101
47	Cu–Ge core–shell nanowire arrays as three-dimensional electrodes for high-rate capability lithium-ion batteries. Journal of Materials Chemistry, 2012, 22, 1511-1515.	6.7	101
48	Shape-Control Fabrication and Characterization of the Airplane-like FeO(OH) and Fe2O3 Nanostructures. Crystal Growth and Design, 2006, 6, 351-353.	1.4	100
49	Selenium Nanotubes Synthesized by a Novel Solution Phase Approach. Journal of Physical Chemistry B, 2004, 108, 1179-1182.	1.2	98
50	Facile Synthesis of Fiveâ€fold Twinned, Starfishâ€like Rhodium Nanocrystals by Eliminating Oxidative Etching with a Chlorideâ€Free Precursor. Angewandte Chemie - International Edition, 2010, 49, 5296-5300.	7.2	97
51	Shape-controlled nanostructured magnetite-type materials as highly efficient Fenton catalysts. Applied Catalysis B: Environmental, 2014, 144, 739-749.	10.8	95
52	Long Bi2S3nanowires prepared by a simple hydrothermal method. Nanotechnology, 2003, 14, 974-977.	1.3	94
53	Nanoscale kinetics of asymmetrical corrosion in core-shell nanoparticles. Nature Communications, 2018, 9, 1011.	5.8	87
54	Lattice-Mismatch-Induced Twinning for Seeded Growth of Anisotropic Nanostructures. ACS Nano, 2015, 9, 3307-3313.	7.3	86

#	Article	IF	CITATIONS
55	Two-dimensional SnS nanosheets fabricated by a novel hydrothermal method. Journal of Materials Science, 2005, 40, 591-595.	1.7	84
56	Preparation and characterization of water-soluble CdS nanocrystals by surface modification of ethylene diamine. Materials Letters, 2005, 59, 1024-1027.	1.3	83
57	Size-controlled synthesis of Pd nanosheets for tunable plasmonic properties. CrystEngComm, 2015, 17, 1833-1838.	1.3	81
58	Inâ€Situ Observation of Hydrogenâ€Induced Surface Faceting for Palladium–Copper Nanocrystals at Atmospheric Pressure. Angewandte Chemie - International Edition, 2016, 55, 12427-12430.	7.2	81
59	Metal Oxide and Sulfide Hollow Spheres: Layer-By-Layer Synthesis and Their Application in Lithium-Ion Battery. Journal of Physical Chemistry B, 2008, 112, 14836-14842.	1.2	78
60	Effects of complexing agent on CdS thin films prepared by chemical bath deposition. Materials Letters, 2004, 58, 5-9.	1.3	77
61	Directional CdS nanowires fabricated by chemical bath deposition. Journal of Crystal Growth, 2002, 246, 108-112.	0.7	75
62	Order-aligned Mn3O4 nanostructures as super high-rate electrodes for rechargeable lithium-ion batteries. Journal of Power Sources, 2013, 222, 32-37.	4.0	75
63	Three-dimensionally porous Fe3O4 as high-performance anode materials for lithium–ion batteries. Journal of Power Sources, 2014, 246, 198-203.	4.0	74
64	From ZnO nanorods to 3D hollow microhemispheres: solvothermal synthesis, photoluminescence and gas sensor properties. Nanotechnology, 2007, 18, 455604.	1.3	73
65	Straight and Thin ZnO Nanorods:Â Hectogram-Scale Synthesis at Low Temperature and Cathodoluminescence. Journal of Physical Chemistry B, 2006, 110, 827-830.	1.2	72
66	Homogeneous coating of Au and SnO2 nanocrystals on carbon nanotubes via layer-by-layer assembly: a new ternary hybrid for a room-temperature CO gas sensor. Chemical Communications, 2008, , 6182.	2.2	72
67	Room temperature electrically pumped ultraviolet random lasing from ZnO nanorod arrays on Si. Optics Express, 2009, 17, 14426.	1.7	71
68	Facile synthesis of Pd–Pt alloy concave nanocubes with high-index facets as electrocatalysts for methanol oxidation. CrystEngComm, 2014, 16, 2411-2416.	1.3	69
69	An In situ TEM study of the surface oxidation of palladium nanocrystals assisted by electron irradiation. Nanoscale, 2017, 9, 6327-6333.	2.8	68
70	Synthesis of Co2SnO4@C core–shell nanostructures with reversible lithium storage. Journal of Power Sources, 2011, 196, 10234-10239.	4.0	66
71	Synthesis of Rhodium Concave Tetrahedrons by Collectively Manipulating the Reduction Kinetics, Facet-Selective Capping, and Surface Diffusion. Nano Letters, 2013, 13, 6262-6268.	4.5	66
72	One-pot, large-scale synthesis of SnO2 nanotubes at room temperature. Chemical Communications, 2008, , 3028.	2.2	65

#	Article	IF	CITATIONS
73	Synthesis of polycrystalline SnO2 nanotubes on carbon nanotube template for anode material of lithium-ion battery. Materials Research Bulletin, 2009, 44, 211-215.	2.7	64
74	Large-scale synthesis of Si@C three-dimensional porous structures as high-performance anode materials for lithium-ion batteries. Journal of Materials Chemistry A, 2014, 2, 20494-20499.	5.2	63
75	Synthesis of ultrafine lanthanum hydroxide nanorods by a simple hydrothermal process. Materials Letters, 2004, 58, 1180-1182.	1.3	62
76	Hydrothermal synthesis, characterization and properties of SnS nanoflowers. Materials Letters, 2006, 60, 2686-2689.	1.3	62
77	Ultrathin Two-Dimensional Pd-Based Nanorings as Catalysts for Hydrogenation with High Activity and Stability. Small, 2015, 11, 4745-4752.	5.2	62
78	Phase-Selective Synthesis and Self-Assembly of Monodisperse Copper Sulfide Nanocrystals. Journal of Physical Chemistry C, 2008, 112, 13390-13394.	1.5	61
79	Novel CuS hollow spheres fabricated by a novel hydrothermal method. Microporous and Mesoporous Materials, 2005, 80, 153-156.	2.2	60
80	Hydrothermal synthesis of flower-like SrCO3 nanostructures. Materials Letters, 2005, 59, 420-422.	1.3	60
81	Layer-stacked tin disulfide nanorods in silica nanoreactors with improved lithium storage capabilities. Nanoscale, 2012, 4, 4002.	2.8	60
82	InOOH Hollow Spheres Synthesized by a Simple Hydrothermal Reaction. Journal of Physical Chemistry B, 2005, 109, 20676-20679.	1.2	59
83	Large-scale synthesis and application of SnS2–graphene nanocomposites as anode materials for lithium-ion batteries with enhanced cyclic performance and reversible capacity. Journal of Alloys and Compounds, 2013, 580, 457-464.	2.8	59
84	Synthesis and Field Emission Characteristics of Bilayered ZnO Nanorod Array Prepared by Chemical Reaction. Journal of Physical Chemistry B, 2005, 109, 17055-17059.	1.2	57
85	Low-Temperature Growth of Uniform ZnO Particles with Controllable Ellipsoidal Morphologies and Characteristic Luminescence Patterns. Journal of Physical Chemistry B, 2006, 110, 19147-19153.	1.2	56
86	Carbon nanotube-based magnetic-fluorescent nanohybrids as highly efficient contrast agents for multimodal cellular imaging. Journal of Materials Chemistry, 2010, 20, 9895.	6.7	56
87	Facile synthesis of uniform MWCNT@Si nanocomposites as high-performance anode materials for lithium-ion batteries. Journal of Alloys and Compounds, 2015, 622, 966-972.	2.8	56
88	Facile synthesis of Rh–Pd alloy nanodendrites as highly active and durable electrocatalysts for oxygen reduction reaction. Nanoscale, 2014, 6, 7012-7018.	2.8	55
89	Cu–Sn Core–Shell Nanowire Arrays as Three-Dimensional Electrodes for Lithium-Ion Batteries. Journal of Physical Chemistry C, 2011, 115, 23620-23624.	1.5	54
90	Synthesis of CdS nanotubes by chemical bath deposition. Journal of Crystal Growth, 2004, 263, 372-376.	0.7	53

#	Article	IF	CITATIONS
91	Atomic resolution liquid-cell transmission electron microscopy investigations of the dynamics of nanoparticles in ultrathin liquids. Chemical Communications, 2013, 49, 10944.	2.2	50
92	CoO/NiSix core–shell nanowire arrays as lithium-ion anodes with high rate capabilities. Nanoscale, 2012, 4, 991-996.	2.8	49
93	Synthesis of cadmium hydroxide nanoflake and nanowisker by hydrothermal method. Materials Letters, 2005, 59, 56-58.	1.3	48
94	Controllable growth of dendrite-like CuO nanostructures by ethylene glycol assisted hydrothermal process. Materials Research Bulletin, 2008, 43, 1291-1296.	2.7	48
95	Cu–Si1â^'xGex core–shell nanowire arrays as three-dimensional electrodes for high-rate capability lithium-ion batteries. Journal of Power Sources, 2012, 208, 434-439.	4.0	48
96	Tuning Surface Structure of Pd ₃ Pb/Pt <i>_n</i> Pb Nanocrystals for Boosting the Methanol Oxidation Reaction. Advanced Science, 2019, 6, 1902249.	5.6	48
97	Strain-Induced Corrosion Kinetics at Nanoscale Are Revealed in Liquid: Enabling Control of Corrosion Dynamics of Electrocatalysis. CheM, 2020, 6, 2257-2271.	5.8	48
98	Self-assembly of CdS: from nanoparticles to nanorods and arrayed nanorod bundles. Materials Chemistry and Physics, 2005, 93, 65-69.	2.0	47
99	Synthesis of La1â^'xCaxMnO3 nanowires by a sol–gel process. Chemical Physics Letters, 2002, 363, 579-582.	1.2	46
100	Formation of PtCuCo Trimetallic Nanostructures with Enhanced Catalytic and Enzyme-like Activities for Biodetection. ACS Applied Nano Materials, 2018, 1, 222-231.	2.4	46
101	In situ study of the growth of two-dimensional palladium dendritic nanostructures using liquid-cell electron microscopy. Chemical Communications, 2014, 50, 9447.	2.2	45
102	Strain-induced Stranski–Krastanov growth of Pd@Pt core–shell hexapods and octapods as electrocatalysts for methanol oxidation. Nanoscale, 2017, 9, 11077-11084.	2.8	43
103	Single-crystalline SnS2nano-belts fabricated by a novel hydrothermal method. Journal of Physics Condensed Matter, 2003, 15, L661-L665.	0.7	42
104	One-Pot Synthesis of Biocompatible CdSe/CdS Quantum Dots and Their Applications as Fluorescent Biological Labels. Nanoscale Research Letters, 2011, 6, 31.	3.1	42
105	A critical SiO _x layer on Si porous structures to construct highly-reversible anode materials for lithium-ion batteries. Chemical Communications, 2017, 53, 6101-6104.	2.2	42
106	High and Fast Response of a Graphene–Silicon Photodetector Coupled with 2D Fractal Platinum Nanoparticles. Advanced Optical Materials, 2018, 6, 1700793.	3.6	42
107	Surface Reconstruction on Uniform Cu Nanodisks Boosted Electrochemical Nitrate Reduction to Ammonia. , 2022, 4, 650-656.		42
108	Assembling CoSn3 nanoparticles on multiwalled carbon nanotubes with enhanced lithium storage properties. Nanoscale, 2011, 3, 1798.	2.8	41

#	Article	IF	CITATIONS
109	Layer-by-layer synthesis of γ-Fe2O3@SnO2@C porous core–shell nanorods with high reversible capacity in lithium-ion batteries. Nanoscale, 2013, 5, 4744.	2.8	41
110	Enhanced activity, durability and anti-poisoning property of Pt/W ₁₈ O ₄₉ for methanol oxidation with a sub-stoichiometric tungsten oxide W ₁₈ O ₄₉ support. Journal of Materials Chemistry A, 2014, 2, 20154-20163.	5.2	41
111	Low-temperature chemical solution route for ZnO based sulfide coaxial nanocables: general synthesis and gas sensor application. Nanotechnology, 2007, 18, 115619.	1.3	39
112	Vertically ordered Ni3Si2/Si nanorod arrays as anode materials for high-performance Li-ion batteries. Nanoscale, 2012, 4, 5343.	2.8	39
113	Carbon Nanotube-ZnO Nanosphere Heterostructures: Low-Temperature Chemical Reaction Synthesis, Photoluminescence, and Their Application for Room Temperature NH ₃ Gas Sensor. Science of Advanced Materials, 2009, 1, 13-17.	0.1	39
114	Sequential occurrence of ZnO nanopaticles, nanorods, and nanotips during hydrothermal process in a dilute aqueous solution. Materials Letters, 2005, 59, 3393-3397.	1.3	38
115	Graphene coupled with Pt cubic nanoparticles for high performance, air-stable graphene-silicon solar cells. Nano Energy, 2017, 32, 225-231.	8.2	38
116	Hydrothermal synthesis of flower-like Bi2S3with nanorods in the diameter region of 30 nm. Nanotechnology, 2004, 15, 1122-1125.	1.3	37
117	Layer-by-layer assembly synthesis of ZnO/SnO2 composite nanowire arrays as high-performance anode for lithium-ion batteries. Materials Research Bulletin, 2011, 46, 2378-2384.	2.7	37
118	Synthesis of Co3O4@SnO2@C core-shell nanorods with superior reversible lithium-ion storage. RSC Advances, 2012, 2, 9511.	1.7	37
119	Facile synthesis of Ru-decorated Pt cubes and icosahedra as highly active electrocatalysts for methanol oxidation. Nanoscale, 2016, 8, 12812-12818.	2.8	37
120	Local epitaxial growth of Au-Rh core-shell star-shaped decahedra: A case for studying electronic and ensemble effects in hydrogen evolution reaction. Applied Catalysis B: Environmental, 2020, 263, 118255.	10.8	37
121	General Solution Route for Nanoplates of Hexagonal Oxide or Hydroxide. Journal of Physical Chemistry B, 2006, 110, 11196-11198.	1.2	36
122	Ni3Si2–Si nanowires on Ni foam as a high-performance anode of Li-ion batteries. Electrochemistry Communications, 2011, 13, 1443-1446.	2.3	36
123	Seed-mediated growth of Au nanorings with size control on Pd ultrathin nanosheets and their tunable surface plasmonic properties. Nanoscale, 2016, 8, 3704-3710.	2.8	36
124	Star-shaped PbS crystals fabricated by a novel hydrothermal method. Journal of Physics Condensed Matter, 2003, 15, 7611-7615.	0.7	35
125	Sonochemical synthesis of amorphous long silver sulfide nanowires. Materials Letters, 2007, 61, 235-238.	1.3	35
126	General Layer-By-Layer Approach To Composite Nanotubes and Their Enhanced Lithium-Storage and Gas-Sensing Properties. Chemistry of Materials, 2009, 21, 5264-5271.	3.2	35

#	Article	IF	CITATIONS
127	Ultrasmall Palladium Nanoclusters as Effective Catalyst for Oxygen Reduction Reaction. ChemElectroChem, 2016, 3, 1225-1229.	1.7	35
128	Labeling transplanted mice islet with polyvinylpyrrolidone coated superparamagnetic iron oxide nanoparticles for <i>in vivo</i> detection by magnetic resonance imaging. Nanotechnology, 2009, 20, 365101.	1.3	34
129	Synthesis of flower-like CdS nanostructures by organic-free hydrothermal process and their optical properties. Materials Letters, 2007, 61, 3507-3510.	1.3	33
130	A Versatile Approach for the Synthesis of ZnO Nanorod-Based Hybrid Nanomaterials via Layer-by-Layer Assembly. Journal of Physical Chemistry C, 2009, 113, 8147-8151.	1.5	33
131	Multimetallic AuPd@Pd@Pt core-interlayer-shell icosahedral electrocatalysts for highly efficient oxygen reduction reaction. Science Bulletin, 2018, 63, 494-501.	4.3	33
132	Tailoring the Edge Sites of 2D Pd Nanostructures with Different Fractal Dimensions for Enhanced Electrocatalytic Performance. Advanced Science, 2018, 5, 1800430.	5.6	33
133	Large-scale synthesis of Ag–Si core–shell nanowall arrays as high-performance anode materials of Li-ion batteries. Journal of Materials Chemistry A, 2014, 2, 13949-13954.	5.2	32
134	Performance Improvement of Graphene/Silicon Photodetectors Using High Work Function Metal Nanoparticles with Plasma Effect. Advanced Optical Materials, 2018, 6, 1701243.	3.6	32
135	Cobalt ferrite nanorings: Ostwald ripening dictated synthesis and magnetic properties. Chemical Communications, 2008, , 5648.	2.2	31
136	Kinetically-controlled growth of cubic and octahedral Rh–Pd alloy oxygen reduction electrocatalysts with high activity and durability. Nanoscale, 2015, 7, 301-307.	2.8	31
137	Controlling the growth and field emission properties of silicide nanowire arrays by direct silicification of Ni foil. Nanotechnology, 2008, 19, 375602.	1.3	30
138	Surface reconstruction engineering of twinned Pd2CoAg nanocrystals by atomic vacancy inducement for hydrogen evolution and oxygen reduction reactions. Applied Catalysis B: Environmental, 2019, 241, 424-429.	10.8	30
139	Single-crystalline Pd square nanoplates enclosed by {100} facets on reduced graphene oxide for formic acid electro-oxidation. Chemical Communications, 2016, 52, 14204-14207.	2.2	29
140	A Mechanistic Study on the Nucleation and Growth of Au on Pd Seeds with a Cubic or Octahedral Shape. ChemCatChem, 2012, 4, 1668-1674.	1.8	28
141	Probing the oxidative etching induced dissolution of palladium nanocrystals in solution by liquid cell transmission electron microscopy. Micron, 2017, 97, 22-28.	1.1	28
142	Nanostructured hybrid cobalt oxide/copper electrodes of lithium-ion batteries with reversible high-rate capabilities. Journal of Alloys and Compounds, 2012, 521, 83-89.	2.8	27
143	Voltage-controlled synthesis of Cu–Li ₂ O@Si core–shell nanorod arrays as high-performance anodes for lithium-ion batteries. Journal of Materials Chemistry A, 2014, 2, 20510-20514.	5.2	27
144	Ultra-small Rh nanoparticles supported on WO _{3â^'x} nanowires as efficient catalysts for visible-light-enhanced hydrogen evolution from ammonia borane. Nanoscale Advances, 2019, 1, 3941-3947.	2.2	27

#	Article	IF	CITATIONS
145	Low temperature chemical reaction synthesis of single-crystalline Eu(OH)3nanorods and their thermal conversion to Eu2O3nanorods. Nanotechnology, 2007, 18, 065605.	1.3	26
146	Large-scale synthesis of silicon arrays of nanowire on titanium substrate as high-performance anode of Li-ion batteries. Journal of Alloys and Compounds, 2012, 526, 53-58.	2.8	26
147	Controlled Growth of Li ₂ O ₂ by Cocatalysis of Mobile Pd and Co ₃ O ₄ Nanowire Arrays for High-Performance Li–O ₂ Batteries. ACS Applied Materials & Interfaces, 2016, 8, 31653-31660.	4.0	26
148	PdCu alloy nanodendrites with tunable composition as highly active electrocatalysts for methanol oxidation. RSC Advances, 2017, 7, 5800-5806.	1.7	26
149	Bimetallic Ni Pd/SBA-15 alloy as an effective catalyst for selective hydrogenation of CO2 to methane. International Journal of Hydrogen Energy, 2019, 44, 13354-13363.	3.8	26
150	A versatile solution route for oxide/sulfide core–shell nanostructures and nonlayered sulfide nanotubes. Nanotechnology, 2005, 16, 2721-2725.	1.3	25
151	Carbon-assisted synthesis of aligned ZnO nanowires. Materials Letters, 2005, 59, 2710-2714.	1.3	25
152	Co/CoO@N-C nanocomposites as high-performance anodes for lithium-ion batteries. Journal of Alloys and Compounds, 2019, 771, 290-296.	2.8	25
153	Sn-Doped Bi ₂ O ₃ nanosheets for highly efficient electrochemical CO ₂ reduction toward formate production. Nanoscale, 2021, 13, 19610-19616.	2.8	25
154	Functionalization of carbon nanotubes with magnetic nanoparticles: general nonaqueous synthesis and magnetic properties. Nanotechnology, 2008, 19, 315604.	1.3	24
155	A General Approach for Uniform Coating of a Metal Layer on MWCNTs via Layer-by-Layer Assembly. Journal of Physical Chemistry C, 2009, 113, 17387-17391.	1.5	24
156	SiGe porous nanorod arrays as high-performance anode materials for lithium-ion batteries. Journal of Alloys and Compounds, 2013, 577, 564-568.	2.8	24
157	Hybrid nanostructures of Au nanocrystals and ZnO nanorods: Layer-by-layer assembly and tunable blue-shift band gap emission. Materials Research Bulletin, 2009, 44, 889-892.	2.7	23
158	Functionalization of ZnO nanorods with γ-Fe2O3 nanoparticles: Layer-by-layer synthesis, optical and magnetic properties. Materials Chemistry and Physics, 2010, 124, 908-911.	2.0	23
159	One-dimensional hybrid nanostructures: synthesis via layer-by-layer assembly and applications. Nanoscale, 2012, 4, 5517.	2.8	23
160	Magnetic-fluorescent nanohybrids of carbon nanotubes coated with Eu, Gd Co-doped LaF3 as a multimodal imaging probe. Journal of Colloid and Interface Science, 2012, 367, 61-66.	5.0	23
161	Synthesis of NixSiy–SiGe core–shell nanowire arrays on Ni foam as a high-performance anode for Li-ion batteries. RSC Advances, 2013, 3, 7713.	1.7	23
162	Synthesis of SiGe-based three-dimensional nanoporous electrodes for high performance lithium-ion batteries. Journal of Power Sources, 2013, 229, 185-189.	4.0	23

#	Article	IF	CITATIONS
163	Mechanistic insight into the synergetic catalytic effect of Pd and MnO2 for high-performance Li–O2 cells. Energy Storage Materials, 2018, 12, 8-16.	9.5	23
164	Firmly bonded graphene–silicon nanocomposites as high-performance anode materials for lithium-ion batteries. RSC Advances, 2015, 5, 46173-46180.	1.7	22
165	Synthesis and characterization of single crystalline MnOOH and MnO2 nanorods by means of the hydrothermal process assisted with CTAB. Materials Letters, 2006, 60, 3895-3898.	1.3	21
166	Facile synthesis of Pd@Ru nanoplates with controlled thickness as efficient catalysts for hydrogen evolution reaction. CrystEngComm, 2018, 20, 4230-4236.	1.3	21
167	Intermetallic Pd ₃ Pb square nanoplates as highly efficient electrocatalysts for oxygen reduction reaction. CrystEngComm, 2019, 21, 290-296.	1.3	21
168	Design of Highly Durable Coreâ ''Shell Catalysts by Controlling Shell Distribution Guided by Inâ€6itu Corrosion Study. Advanced Materials, 2021, 33, e2101511.	11.1	21
169	A simple and novel low-temperature hydrothermal synthesis of ZnO nanorods. Inorganic Materials, 2006, 42, 1210-1214.	0.2	20
170	Improved cyclic stability of Mg2Si by direct carbon coating as anode materials for lithium-ion batteries. Journal of Alloys and Compounds, 2014, 587, 807-811.	2.8	20
171	Embedding Ultrafine and High ontent Pt Nanoparticles at Ceria Surface for Enhanced Thermal Stability. Advanced Science, 2017, 4, 1700056.	5.6	20
172	Some critical factors in the synthesis of CdS nanorods by hydrothermal process. Materials Letters, 2005, 59, 3037-3041.	1.3	19
173	Electrochemical synthesis of SnCo alloy shells on orderly rod-shaped Cu current collectors as anode materials for lithium-ion batteries with enhanced performance. Journal of Alloys and Compounds, 2013, 570, 119-124.	2.8	19
174	Sub-2 nm SnO2 nanocrystals: A reduction/oxidation chemical reaction synthesis and optical properties. Materials Research Bulletin, 2008, 43, 3164-3170.	2.7	17
175	Growth and photoelectrochemical properties of ordered CuInS2 nanorod arrays. Chemical Communications, 2012, 48, 4746.	2.2	17
176	Ion-templated fabrication of Pt-Cu alloy octahedra with controlled compositions for electrochemical detection of H2O2. Journal of Alloys and Compounds, 2019, 788, 1334-1340.	2.8	17
177	Unexpected Kirkendall effect in twinned icosahedral nanocrystals driven by strain gradient. Nano Research, 2020, 13, 2641-2649.	5.8	17
178	Phase-controlled synthesis of nickel silicide nanostructures. Materials Research Bulletin, 2012, 47, 3797-3803.	2.7	16
179	Detection of viability of transplanted beta cells labeled with a novel contrast agent – polyvinylpyrrolidoneâ€coated superparamagnetic iron oxide nanoparticles by magnetic resonance imaging. Contrast Media and Molecular Imaging, 2012, 7, 35-44.	0.4	16
180	Silver–nickel oxide core–shell nanoflower arrays as high-performance anode for lithium-ion batteries. Journal of Power Sources, 2015, 285, 131-136.	4.0	16

#	Article	IF	CITATIONS
181	Intermetallic Pd ₃ Pb ultrathin nanoplate-constructed flowers with low-coordinated edge sites boost oxygen reduction performance. Nanoscale, 2019, 11, 17301-17307.	2.8	16
182	Facile synthesis of high-quality Pt nanostructures with a controlled aspect ratio for methanol electro-oxidation. CrystEngComm, 2014, 16, 8340-8343.	1.3	15
183	Porous Si@C coaxial nanotubes: layer-by-layer assembly on ZnO nanorod templates and application to lithium-ion batteries. CrystEngComm, 2017, 19, 1220-1229.	1.3	15
184	Cathodoluminescence and its mapping of flower-like ZnO, ZnO/ZnS core–shell and tube-like ZnS nanostructures. Materials Research Bulletin, 2007, 42, 1286-1292.	2.7	14
185	Facile synthesis of PtCu ₃ alloy hexapods and hollow nanoframes as highly active electrocatalysts for methanol oxidation. CrystEngComm, 2016, 18, 7823-7830.	1.3	14
186	Magnesium catalyzed growth of SiO2hierarchical nanostructures by a thermal evaporation process. Nanotechnology, 2008, 19, 165601.	1.3	13
187	Seed-mediated synthesis of Au@PtCu nanostars with rich twin defects as efficient and stable electrocatalysts for methanol oxidation reaction. RSC Advances, 2019, 9, 35887-35894.	1.7	13
188	Facile synthesis of ternary PtPdCu alloy hexapods as highly efficient electrocatalysts for methanol oxidation. RSC Advances, 2020, 10, 12689-12694.	1.7	13
189	A unique ligand effect in Pt-based core–shell nanocubes to boost oxygen reduction electrocatalysis. Journal of Materials Chemistry A, 2021, 9, 22653-22659.	5.2	13
190	Garnet Electrolytes with Ultralow Interfacial Resistance by SnS ₂ Coating for Dendrite-Free all-Solid-State Batteries. ACS Applied Energy Materials, 2021, 4, 2873-2880.	2.5	13
191	Surface faceting and compositional evolution of Pd@Au core–shell nanocrystals during <i>in situ</i> annealing. Physical Chemistry Chemical Physics, 2019, 21, 3134-3139.	1.3	12
192	Transformation mechanism of Te particles into Te nanotubes and nanowires during solvothermal process. Journal of Crystal Growth, 2006, 289, 568-573.	0.7	11
193	Cobalt–iron cyanide hollow cubes: Three-dimensional self-assembly and magnetic properties. Journal of Alloys and Compounds, 2011, 509, 8382-8386.	2.8	11
194	Solvothermal synthesis of carbon-coated tin nanorods for superior reversible lithium ion storage. Materials Research Bulletin, 2011, 46, 2278-2282.	2.7	11
195	A novel low-temperature chemical solution route for straight and dendrite-like ZnO nanostructures. Materials Science and Engineering B: Solid-State Materials for Advanced Technology, 2007, 141, 76-81.	1.7	10
196	Synthesis of nanoporous three-dimensional current collector for high-performance lithium-ion batteries. RSC Advances, 2013, 3, 7543.	1.7	10
197	Strain effect in Pd@PdAg twinned nanocrystals towards ethanol oxidation electrocatalysis. Nanoscale Advances, 2021, 4, 111-116.	2.2	10
198	Large-scale synthesis of water-soluble nanowires as versatile templates for nanotubes. Chemical Communications, 2011, 47, 1006-1008.	2.2	9

#	Article	IF	CITATIONS
199	Controllable chemical reaction synthesis of Tb(OH)3 nanorods and their photoluminescence property. Materials Letters, 2009, 63, 1180-1182.	1.3	8
200	Monitoring the shape evolution of Pd nanocubes to octahedra by PdS frame markers. Nanoscale, 2014, 6, 3518-3521.	2.8	8
201	Core–shell and alloy integrating PdAu bimetallic nanoplates on reduced graphene oxide for efficient and stable hydrogen evolution catalysts. RSC Advances, 2017, 7, 43373-43379.	1.7	8
202	Designed Synthesis of CoO/CuO/rGO Ternary Nanocomposites as High-Performance Anodes for Lithium-Ion Batteries. Jom, 2018, 70, 1793-1799.	0.9	8
203	Controlled oxidative etching of gold nanorods revealed through in-situ liquid cell electron microscopy. Science China Materials, 2020, 63, 2599-2605.	3.5	8
204	PdPtRu nanocages with tunable compositions for boosting the methanol oxidation reaction. Nanoscale Advances, 2022, 4, 1158-1163.	2.2	8
205	Flower-like silicon nanostructures. Physica E: Low-Dimensional Systems and Nanostructures, 2007, 38, 27-30.	1.3	7
206	Controllable growth of Se nanotubes and nanowires from different solvent during the sonochemical process. Materials Letters, 2009, 63, 1-4.	1.3	7
207	Silver-nickel oxide core-shell nanoparticle array electrode with enhanced lithium-storage performance. Electrochimica Acta, 2015, 174, 893-899.	2.6	7
208	A novel Co–Li ₂ O@Si core–shell nanowire array composite as a high-performance lithium-ion battery anode material. Nanoscale, 2016, 8, 4511-4519.	2.8	7
209	Wet etching in β-Ga ₂ O ₃ bulk single crystals. CrystEngComm, 2022, 24, 1127-1144.	1.3	7
210	Enhanced electrocatalytic reduction of CO ₂ to formate <i>via</i> doping Ce in Bi ₂ O ₃ nanosheets. Nanoscale Advances, 2022, 4, 2288-2293.	2.2	7
211	Revealing the elemental-specific growth dynamics of Pt–Cu multipods by scanning transmission electron microscopy and chemical mapping. Journal of Materials Chemistry A, 2015, 3, 21284-21289.	5.2	6
212	Facile synthesis of Au@PNIPAMâ€ <i>b</i> â€PPy nanocomposites with thermosensitive and photothermal effects. Journal of Polymer Science Part A, 2016, 54, 3079-3085.	2.5	6
213	Morphology and phase selective synthesis of EuF3 nanostructures by polyelectrolyte assisted chemical reaction and their optical properties. Materials Chemistry and Physics, 2009, 115, 562-566.	2.0	5
214	Large-scale synthesis of water-soluble Na2SiF6 nanotubes with polyacrylic acid as a surfactant. Materials Research Bulletin, 2012, 47, 3923-3926.	2.7	5
215	Twinned silicon and germanium nanocrystals: Formation, stability and quantum confinement. AIP Advances, 2015, 5, .	0.6	5
216	Developing an aqueous approach for synthesizing Au and M@Au (M = Pd, CuPt) hybrid nanostars with plasmonic properties. Physical Chemistry Chemical Physics, 2015, 17, 1265-1272.	1.3	5

#	Article	IF	CITATIONS
217	Au-Doped intermetallic Pd ₃ Pb wavy nanowires as highly efficient electrocatalysts toward the oxygen reduction reaction. CrystEngComm, 2020, 22, 6478-6484.	1.3	5
218	Gaâ€Ðoped Intermetallic Pd3Pb Nanocubes as a Highly Efficient and Durable Oxygen Reduction Reaction Electrocatalyst. ChemistrySelect, 2021, 6, 3891-3896.	0.7	5
219	Facile Synthesis of Pd@PtM (M = Rh, Ni, Pd, Cu) Multimetallic Nanorings as Efficient Catalysts for Ethanol Oxidation Reaction. Frontiers in Chemistry, 2021, 9, 683450.	1.8	5
220	Tailor of ZnO morphology by heterogeneous nucleation in the aqueous solution. Materials Research Bulletin, 2007, 42, 1316-1322.	2.7	4
221	Size-controlled synthesis of Au nanorings on Pd ultrathin nanoplates as efficient catalysts for hydrogenation. CrystEngComm, 2017, 19, 6588-6593.	1.3	4
222	Enhanced oxygen reduction activity of Pt shells on PdCu truncated octahedra with different compositions. RSC Advances, 2018, 8, 34853-34859.	1.7	4
223	Facile Synthesis of PdCuRu Porous Nanoplates as Highly Efficient Electrocatalysts for Hydrogen Evolution Reaction in Alkaline Medium. Metals, 2021, 11, 1451.	1.0	4
224	Synthesis and characterization of CdS based sulfide coaxial cable and nanotubes by sacrificial approach. Materials Letters, 2006, 60, 2004-2008.	1.3	3
225	Facile synthesis of PdSn alloy octopods through the Stranski–Krastanov growth mechanism as electrocatalysts towards the ethanol oxidation reaction. CrystEngComm, 2022, 24, 3230-3238.	1.3	3
226	Synthesis of One-Dimensional Chalcogenides by a Novel Hydrothermal Process. Solid State Phenomena, 2004, 99-100, 203-208.	0.3	2
227	Spherical to truncated octahedral shape transformation of palladium nanocrystals driven by e-beam in aqueous solution. Nano Research, 2019, 12, 2623-2627.	5.8	2
228	Morphology Control of PbS Nanocrystals by a Novel Hydrothermal Process. Solid State Phenomena, 2004, 99-100, 197-202.	0.3	1
229	Hydrofluoric acid free synthesis of macropores on silicon by chemical vapor deposition and their photoluminescence. Physica E: Low-Dimensional Systems and Nanostructures, 2008, 40, 494-498.	1.3	0
230	Quantum dots decorated single walled carbon nanotubes for multimodal cellular imaging. , 2010, , .		0
231	Low temperature synthesis of SnSr(OH)6 nanoflowers and photocatalytic performance for organic pollutants. International Journal of Materials Research, 2022, 113, 80-90.	0.1	0